

Design and Analysis of ZCS based Efficient DC-DC Boost Converter for the Non-Conventional power units with CV/CC control

Kathirvelan.J¹, Viswarani.C.D²

¹MEMS & Sensors Division, VIT University, Vellore, T.N., India.

²Department of Electrical Engineering, Saraswathi Velu College of Engineering, Sholingur, T.N., India

¹E-mail : j.kathirvelan@vit.ac.in, ¹Mobile :9500356597

ABSTRACT

The analysis of high efficiency DC-DC boost converter with zero current switching (ZCS) and constant voltage/current (CV/CC) control technology for the application of non-conventional power units (NCPU) on simulation basis is presented in this paper. The significance of this converter is based on the energy recovery system. The proposed converter does not consider the leakage inductance of the transformer as a drawback and instead it uses it for efficient energy transfer, thus avoiding problems of low efficiency, voltage regulation and waveform distortions. Apart from these advantages the proposed converter has some more features like zero current switching and elimination of separate filter inductor there by optimizing the cost and size of the converter unit.

KEY WORDS

High efficiency DC-DC boost converter, ZCS, NCPU, Energy recovery system, Leakage inductance.

1. INTRODUCTION

This high efficiency DC – DC boost converter is proposed to use in the Non-Conventional Power Units (NCPU)[1-4]. The block diagram of is shown in figure 1. The main functional components of this NCPU is a solar cells, DC-DC converter and an inverter with 230V and 50Hz output.

In order to get an output of 230V from the inverter, we require at least 350 volts DC supply. This high DC source can not be sourced in the remote applications. So it needs a booster for boosting a voltage of (20-30)V obtained from the solar cells[1].

This boosting can also be done by using an ordinary boost converters which suffers from lowered efficiency due to high duty ratio maintained for obtained high dc voltage as an output. As per the experimental data the average efficiency of these converters will be approximately 40% to 50% only[1].

Even we can go for push pull or full bridge converters configurations to overcome these problems but again the large turns ratio maintained in the booster transformers offers very high leakage reactance. This leakage reactance effect again produces low efficiency due to reactive power consumption and also waveform distortion and finally voltage instability even though good controllers are used [1,2].

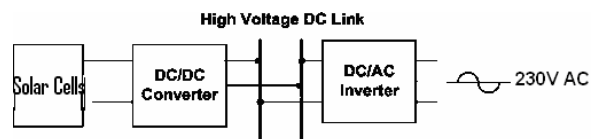


Fig.1 Typical layout of NCPU

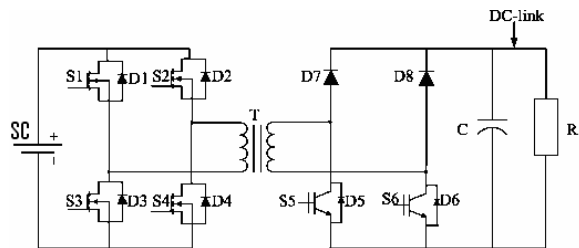


Fig. 2: Topology of the proposed DC-DC converter.

Fig.2 represents the topology of the proposed converter which can overcome the problems highlighted in all the above said converters.

This converter can yield an overall efficiency of about 90% and cost will be reduced as some of the filter components can be eliminated [1]. The transformer is operated at high frequency so the cost as well as size of the transformer can be reduced. So all together the proposed converter has high efficiency, economical and compatible.

2. PROPOSED DC-DC CONVERTER

2.(A). Topology:

Fig. 2 shows the topology of the proposed converter, where FC is the low voltage fuel cell, S1-S6 are active switches, D1-D6 are body diodes of switches S1-S6, respectively, D7 and D8 are power diodes, C is the filter capacitor, T is the transformer, and R is the load of the dc-dc converter.

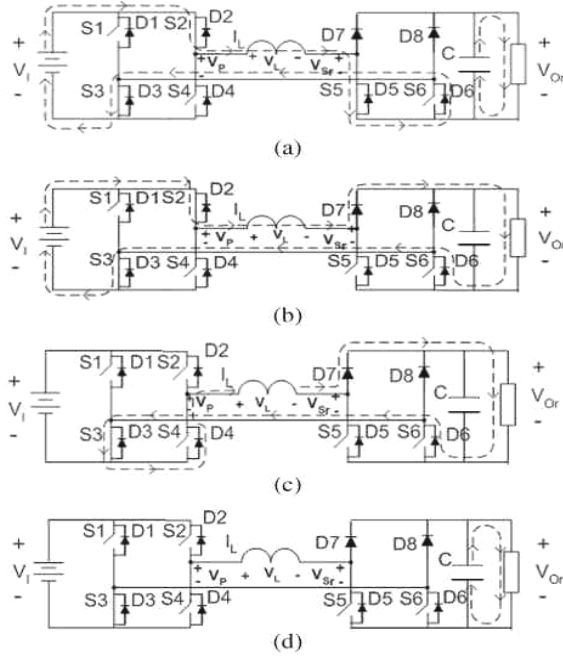


Fig.3. Transformer primary side referred equivalent circuits of the converter during different time periods in the first half cycle: (a) t_0-t_1 , (b) t_1-t_2 , (c) t_2-t_3 , and (d) t_3-t_4 .

2.(B). Operation:

The transformer primary side referred equivalent circuits of the converter are shown in Fig. 3 and are used to explain the operation of the converter. The magnetizing inductance of the transformer is ignored and only the leakage inductance is considered in the derivation of the equivalent circuits. The waveforms of key components of the converter in one complete cycle are shown in Fig. 4.

In Figs. 3 and 4, V_i , V_{Or} , V_p , V_{Sr} , V_L , and I_L

stand for the input voltage of the converter, output voltage of the converter (primary side referred), primary side voltage of the transformer, secondary side voltage of the transformer (primary side referred), voltage across the leakage inductance of the transformer (primary side referred), and primary side current of the transformer, respectively.

In Fig. 4, G_1-G_6 represent the gating signals to switches S1-S6, respectively, and the time period from t_0-t_8 represents a complete operating cycle of the converter. As shown in Fig. 4, the operation of the converter in the second half cycle, from t_4-t_8 , is similar to that in the first half cycle, from t_0-t_4 , except being in the opposite direction. Therefore, only the operation of the converter in the first half cycle, from t_0-t_4 , is detailed and illustrated in Fig. 3(a)-(d).

The operation of the converter during different time periods in the first half cycle is explained as follows.

[t_0-t_1]: Switches S_2 , S_3 , and S_5 are gated. A closed current path is created as shown in Fig. 3(a). One can easily derive that $V_p = V_i$, $V_{Sr} = 0$ and

$$V_L = (V_p - V_{sr}) = (V_i - 0) = V_i$$

Using $V_L = V_i$ and $V_L = L(dI_L/dt)$, where L is the leakage inductance of the transformer, one can derive

$$I_L = \frac{V_i}{L} t. \quad \text{Eqn.(1)}$$

It should be noted that S2, S3, and S5 are turned on at zero current condition.

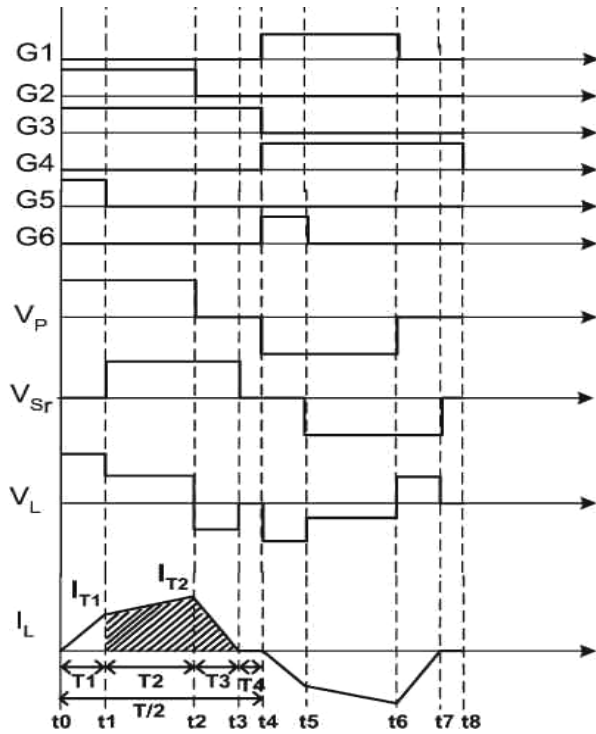


Fig. 4. Waveforms of key components of the converter in one complete cycle.

[t₁-t₂]: Switches S₂ and S₃ are kept on while switch S₅ is turned off. D₇ conducts to carry the inductor current as a result of the turn-off of S₅. A closed current path is created as shown in Fig. 3(b). One can derive that $V_p = V_i$, $V_{sr} = V_{or}$ and $V_L = V_p - V_{sr} = V_i - V_{or}$. Similar to Eqn. (1), one can have

$$I_L = I_{T2} = \frac{V_i - V_{or}}{L} t + I_{T1} \quad \text{Eqn.(2)}$$

where I_{T1} is the current through the

transformer at time instant t₁, and can be calculated using (1). As a result, the current in the transformer continues to rise linearly, but now at a slower rate, as is shown in Fig. (4).

[t₂-t₃]: Switch S₂ is turned off while S₃ is kept on. D₄ conducts to carry the inductor current as a result of the turn-off of S₂. The inductor current flows as shown in Fig 3(c) and is given as

$$I_L = I_{T2} - \frac{V_{or}}{L} t \quad \text{Eqn.(3)}$$

where I_{T2} is the current through the transformer at time instant t₂, and can be calculated using Eqn.(2).

[t₃-t₄]: No current or energy flow in the converter. S₃ is turned off at $t = t_4$. It should be noted that S₃ is turned off at zero current condition. The proposed converter is operated at a fixed switching frequency. As can be seen from the description of the working of the converter, time periods T₁ and T₂ control the current through the transformer and hence the power of the converter. It can also be seen that switches S₅ and S₆ are turned on for time period T₁, with a 180° phase difference. Switches S₁ and S₂ are turned on for a time period equal to T₁ + T₂, with a 180° phase difference. And switches S₃ and S₄ are turned on for half of the switching time period (T/2), with a 180° phase difference.

2.(C). Control:

The control strategy of the proposed converter is shown in Fig. 5. The output voltage of the converter is sensed and compared to the reference voltage (V_{oref}). The voltage error thus obtained is passed through a proportional-integral (PI) controller to obtain the reference output (2) current (I_{oref}). The output current I_o is sensed and compared to the I_{oref} . The current error thus obtained is passed through

two different PI circuits. The signals thus obtained are compared to a high frequency (equal to switching frequency) saw tooth signal to generate pulse-width modulated (PWM) control signals with pulse widths T_1 and $T_1 + T_2$. A constant value signal is also compared to the same saw tooth signal to generate PWM control signal with pulse width $T/2$. These three PWM control signals of pulse width T_1 , $T_1 + T_2$, and $T/2$ are individually phase delayed by 180° to obtain three more PWM control signals.

Thus a total of six PWM control signals are obtained which are used to control the six active switches of the proposed converter, as indicated in Fig. 5.

3. RESULTS

Performance of the proposed converter is simulated on a open loop for a fixed operating point of 20Volts input voltage and an output voltage 250Volts DC.

The simulation results are shown in Fig. 5, where from top to bottom is primary side voltage (V_p), secondary side voltage (V_s), transformer primary current (I_L) and output voltage V_{dc} . As shown in Fig. 6, during time period T_1 , all switches S_2 , S_3 , and S_5 are on, V_p is positive and $V_s = 0$. Thus, the current through the transformer rises linearly.

During time period T_2 , S_5 is turned off and S_2 and S_3 are kept on. Both V_p and V_{sr} are positive, but $V_p > V_{sr}$, where V_{sr} is the secondary side voltage referred to the primary side. Therefore, the current through the transformer continues to rise, but at a very slow rate (because of small difference between V_p and V_s). During time period T_3 , switch S_2 is switched off and only switch S_3 is on. Now V_s is positive and $V_p = 0$. The transformer current starts to fall and falls

until it reaches zero. During time period T_4 , all three switches are off, V_p and V_s both are zero, and there is no current through the transformer. Thus, by comparing Fig. 6 to Fig. 4, it is seen that the simulated results match the designed waveforms, and thus the proposed converter working is verified by simulation.

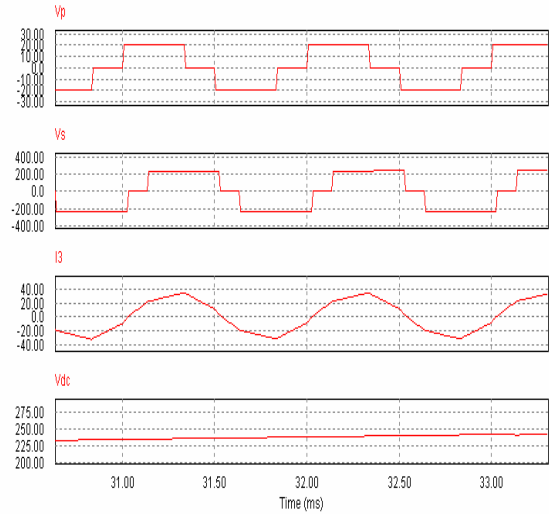


Fig.5: Primary voltage, Secondary voltage, Transformer primary current and output DC voltage

3. (A). Constant Voltage Control:

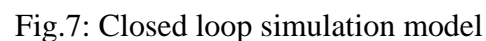
The closed-loop performance of the proposed converter is also investigated by simulation and the results are shown in Figs 7, 8, 9, 10. Before $t = 0.3s$, the converter is in a stable state with the output voltage at 350 V and the output current equals to 1 Amps. The fuel cell voltage is 20 V and the fuel cell current is 34Amps Avg.

At time instant $t = 0.5s$ the input voltage is stepped up to 25Volts from 20Volts initial condition. It can be seen that the output voltage is maintained at 350 V constantly and the load current also settled at 1Amps. The fuel cell average current is increased from 34Amps to 52Amps as duty ratio is reduced to maintain the output voltage constantly.

the simulation that the proposed converter can maintain designed output voltage when the input voltage changes within the specified limits as well for the load change.



The simulation model of the proposed converter in the closed loop configuration is designed by using Simulink model of MatLab 7.0 and it is given in the fig. 7



3.(A).2.Simulation Result:

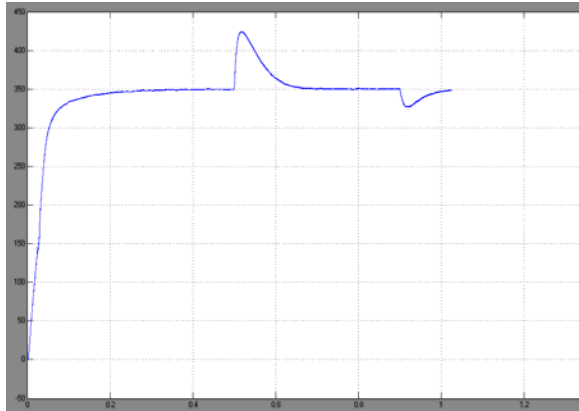


Fig 8: Output DC voltage on closed loop configuration.

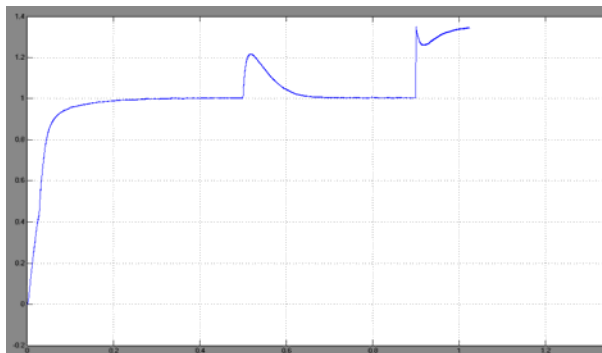


Fig 9: Output load current on closed loop configuration.

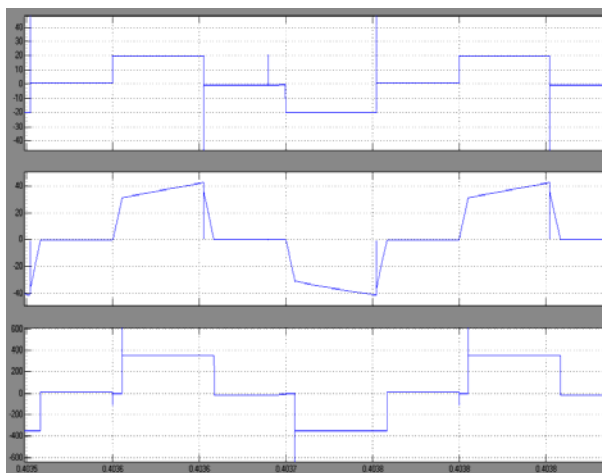


Fig 10: Transformer primary voltage,

current and secondary voltage on closed loop configuration.

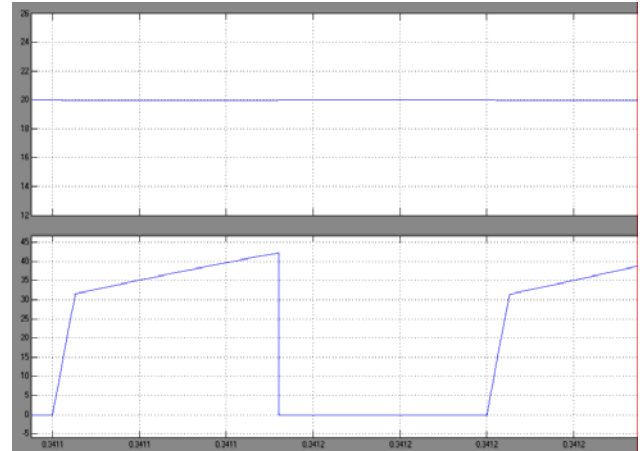


Fig 11: Fuel cell voltage and current on closed loop configuration

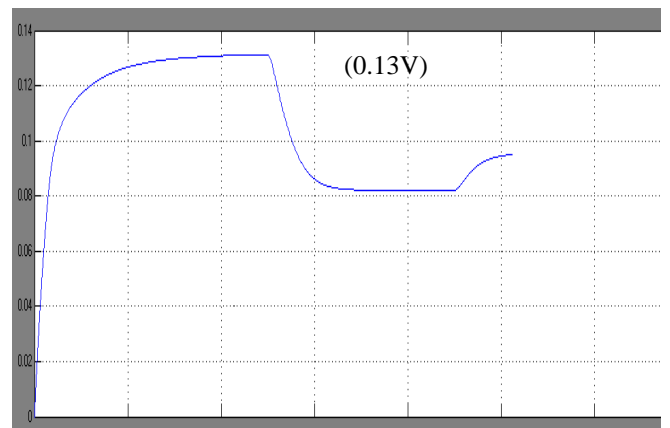


Fig. 12: PI controller output.

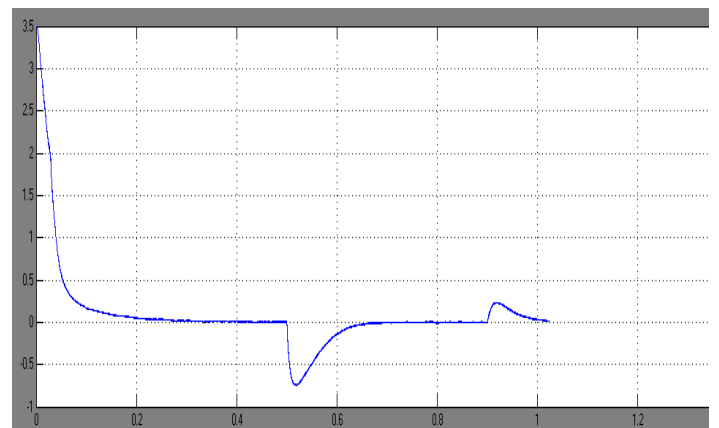


Fig. 13: Error signal waveform

3. (B). Constant Current Control:

Apart from controlling and regulating the output voltage at various different levels, even the current handled by the converter also can be controlled as required by introducing constant current control technique. An additional current loop is introduced along with voltage loop for regulating the current. Both the voltage loop and current loop will work together as logical OR gate circuit. Normally the circuit can be operated in the voltage mode, but the current mode will be activated when ever the constant current regulation is required.

3.(B).1.Advantage of Constant Current Control:

Apart from the constant voltage regulation even the current also can be regulated constantly at different values. The converter can also be operated as a multiple current control converter. It limits the maximum value of current that is drawn from the converter to the load. It also acts as a short circuit protection for the converter and protects the load from drawing high currents

3.(B).2.Application of Constant Current Control:

The converter which is embedded with constant voltage and constant current control can be used very effectively for sensitive loads. It can also be used for system automation. This power supplies can be used for speed control operations. This converter can be used very effectively to check the dynamic performance of various loads.

3.(B).3.Simulation Model:

The simulation model of the proposed converter is designed by using Simulink model of MatLab 7.0 software and it is given in the fig. 14

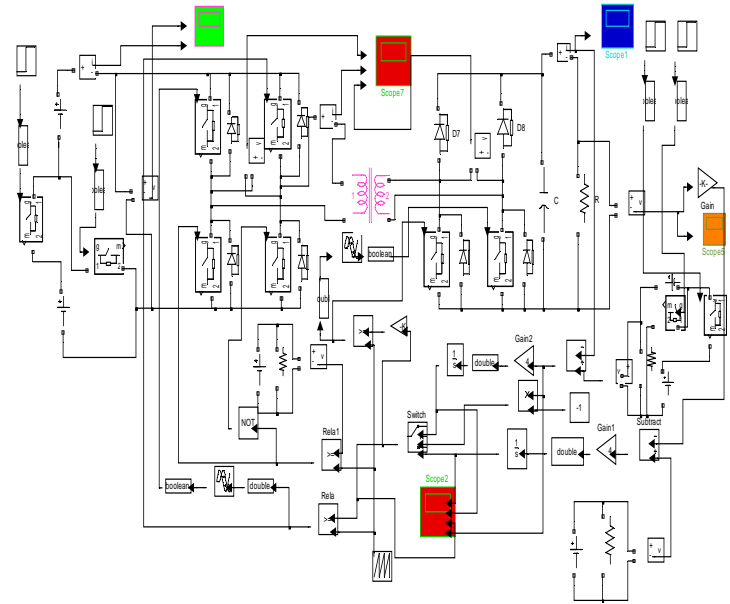


Fig. 14: Simulation model of constant current control.

3.(B).4.Simulation Result:

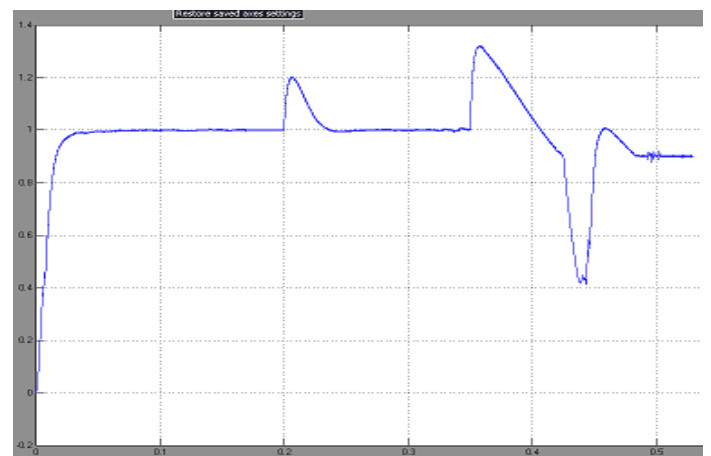


Fig. 15: Constant Current of 0.9Amps

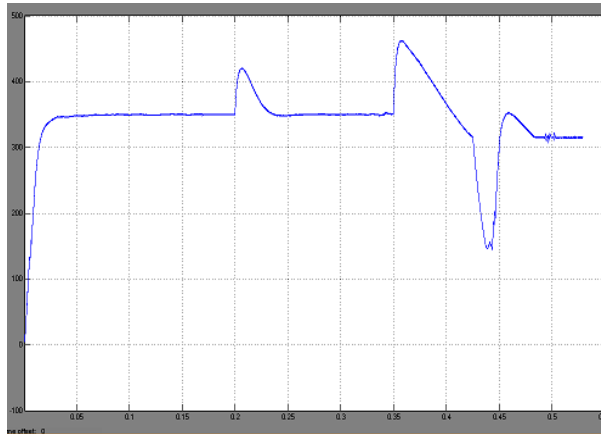


Fig. 16: Output Voltage at 0.9Amps current limitation.

4. DISCUSSION

From the simulated results, it is observed the following values of input and output voltages/currents:

Input Voltage : 20 Volts DC

Input Current : 18.75Amps

Input Power : 375 Watts

Output Voltage: 350Volts DC

Output Current : 1Amps

Output Power : 350Watts

$$\begin{aligned} \% \text{ Efficiency} &= \left[\frac{\text{Output Power}}{\text{Input Power}} \right] \times 100 \\ &= [350/375] \times 100 \\ &= 93.33\% \end{aligned}$$

So when the efficiency of the proposed converter is compared with the normal existing converters, it is very much on the higher side.

5.CONCLUSION

The proposed ZCS based DC–DC converter for the non-conventional power units is designed and analyzed for it's suitability for the power units by simulation. The leakage inductance of the transformer is used for

energy conversion. This not only mitigates the low efficiency and difficulty in a control problem resulting from the leakage inductance but also eliminates the need for a separate filter inductor. Soft switching is achieved to reduce the switching losses. The real time analysis of this converter using hardware will provide more accurate performance of this converter and it will enhance the application of this converter in the non-conventional power units. The next phase of the research work will be the implementation of NCPU in real time applications and validation of performance.

REFERENCES:

- 1.Rahul sharma, Hongwei Gao, Low cost high efficiency dc-dc converter for fuel cell powered auxiliary power unit of a heavy vehicle, IEEE Trans., 2006,Vol.21, No3, pp.587-591.
2. Hui Li and Zheng Peng, A natural ZVS medium-power bidirectional dc-dc converter with minimum number of devices, IEEE Trans., 2003, Vol.39, No2, pp.525-535.
3. Fang Z.Peng and Hui Li, A new ZVS bidirectional dc-dc converter for fuel cell and battery application, IEEE Trans., 2004, vol.19, No.1.pp. 54-65.
4. Dylan Dah-Chaun, Herbert Ho-Ching, A single stage AC/DC converter with high power factor, regulated bus voltage and output voltage, IEEE Trans., 2008, vol.23, No.1.pp.218-228.